

Depletion in fermionic chains with inhomogeneous hoppings

Begoña Mula,^{1,2} Nadir Samos Sáenz de Buruaga,³ Germán Sierra,⁴ Silvia N. Santalla,⁵ and Javier Rodríguez-Laguna¹

¹*Dto. Física Fundamental, Universidad Nacional de Educación a Distancia (UNED), Madrid, Spain*

²*Dto. Matemáticas, Universidad Carlos III de Madrid, Leganés, Spain*

³*Instituto de Nanociencia y Materiales de Aragón (INMA), CSIC-Universidad de Zaragoza, Zaragoza, Spain*

⁴*Instituto de Física Teórica UAM/CSIC, Universidad Autónoma de Madrid, Cantoblanco, Madrid, Spain*

⁵*Dto. Física & GISC, Universidad Carlos III de Madrid, Leganés, Spain*

(Dated: September 19, 2022)

The ground state of a free-fermionic chain with inhomogeneous hoppings at half-filling can be mapped into the Dirac vacuum on a static curved space-time, which presents exactly homogeneous occupations due to particle-hole symmetry. Yet, far from half-filling we observe density modulations and depletion effects. The system can be described by a 1D Schrödinger equation on a different static space-time, with an effective potential which accounts for the depleted regions. We provide a semiclassical expression for the single-particle modes and the density profiles associated to different hopping patterns and filling fractions. Moreover, we show that the depletion effects can be compensated for all filling fractions by adding a chemical potential proportional to the hoppings. Interestingly, we can obtain exactly the same density profiles on a homogeneous chain if we introduce a chemical potential which is inverse to the hopping intensities, even though the ground state is different from the original one.

I. INTRODUCTION

Free fermionic chains are one of the most relevant basic models of quantum many-body physics. Beyond its relevance in condensed matter physics, they constitute one of the basic structures behind quantum simulators [1, 2], which promise to help understand many interesting phenomena. For example, fermionic chains have been put forward to simulate the Dirac vacuum in curved space-times, which would lead us to perform experiments on the Unruh effect or Casimir forces on a background gravitational field [3–5]. Such quantum simulators can be built using ultracold fermionic atoms on an optical lattice, employing modulated laser beams to provide inhomogeneous hopping amplitudes between neighboring cells [6]. The key insight is that an inhomogeneity in the hoppings will give rise to an effective space-time metric in the thermodynamic limit, under some mild conditions.

In the aforementioned examples the Dirac vacuum is obtained as the ground state (GS) of the lattice Hamiltonian at half-filling. Interestingly, when the underlying lattice is bipartite the system presents particle-hole symmetry and the occupation numbers become exactly homogeneous. Moreover, its large scale physical properties can be accounted for using conformal invariance arguments on the appropriately deformed metric [7–11]. Yet, as the filling fraction is lowered (or raised) the density will vary from point to point. Moreover, it may become negligible in the region containing the lowest hopping amplitudes, a phenomenon which we have termed *depletion*. This result can be readily understood in the strong inhomogeneity regime, employing a strong-disorder renormalization group (SDRG) scheme [12], because the orbitals with the lowest energies are localized upon the lowest hopping amplitudes, which may correspond sometimes to effective long-distance renormalized bonds. An illustration of this situation can be seen in Fig. 1. Yet, in the

weak inhomogeneity limit the mathematical description of the depletion effects faces some technical challenges: second-order derivatives of the fields must be considered in the gradient expansion of the Hamiltonian, thus breaking explicitly the conformal symmetry which characterizes the half-filling case.

This depletion has already been observed by other authors. For example, it has been reported that the entanglement entropies of inhomogeneous fermionic chains away from half-filling can be interpreted as those corresponding to an effective shorter chain, corresponding to the non-depleted region [13]. Moreover, the effect of a finite density fermion field in entanglement has been studied both in the relativistic [14] and non-relativistic frameworks [15].

This work addresses the emergence of depletion in inhomogeneous pure-hopping free fermionic chains away from half-filling, and it is divided as follows. In Sec. II we describe our physical model, while Sec. III describes the depletion phenomenon in the strong disorder limit. Sec. IV describes our continuum approximation for all filling fractions, and the effective Schrödinger equation on a different space-time metric. Sec. V describes our theoretical approach to the density profiles and the depleted areas. The question of the effective potential is addressed in Sec. VI, showing that it can be either proportional to the hopping amplitudes or inversely proportional to them, depending on our precise definition. Finally, Sec. VII summarizes our findings and discusses our suggestions for further work.

II. MODEL

Let us consider an open fermionic chain with N (even) sites, whose Hilbert space is spanned by creation operators c_i^\dagger , $i \in \{1, \dots, N\}$ following standard anticommu-

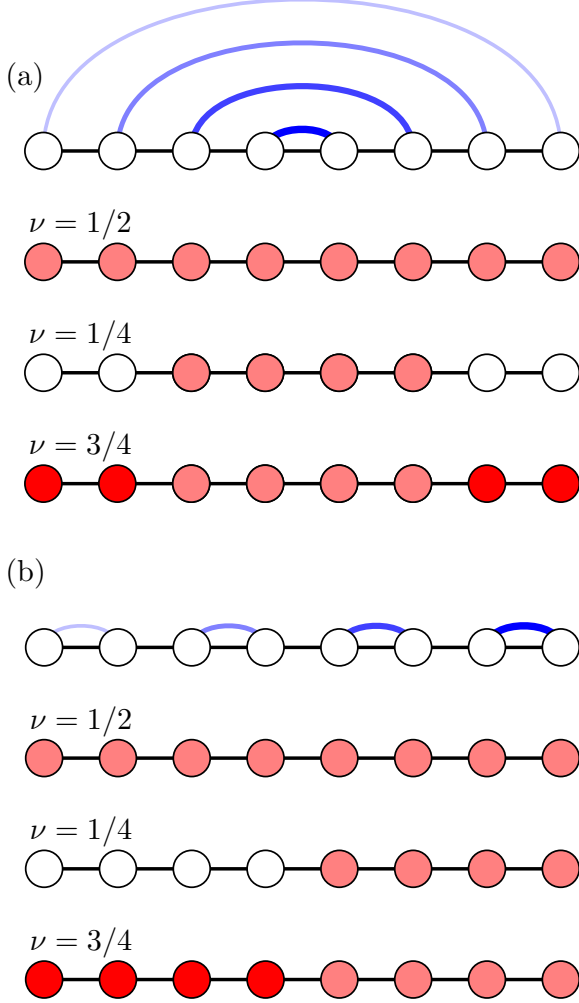


FIG. 1. Depletion in free-fermionic chains with inhomogeneous hoppings, explained using the SDRG for different values of the filling fraction ν . In (a) we have a rainbow chain whose single-particle orbitals are bonds between symmetrically placed sites. For $\nu = 1/2$, all the bonds get single occupation (light red) and the density is exactly homogeneous. For $\nu = 1/4$ we only occupy the two strongest bonds, leaving a depleted area near the borders. For $\nu = 3/4$ the weakest bonds get double occupation (bright red), while the strongest remain with single occupation. In (b) we have a dimerized chain such that the energy associated to each bond grows rightwards. For $\nu = 1/2$ we obtain the same homogeneous density. For $\nu = 1/4$ only the rightmost bonds are occupied, and the left half is depleted. For $\nu = 3/4$ the leftmost bonds obtain double occupation, and the rightmost ones still get one particle.

tation relations, $\{c_i^\dagger, c_j\} = \delta_{i,j}$. We define an inhomogeneous hopping Hamiltonian,

$$H(\mathbf{J})_N = - \sum_{i=1}^{N-1} J_i c_i^\dagger c_{i+1} + \text{h.c.}, \quad (1)$$

where $\mathbf{J} = \{J_i\}_{i=1}^{N-1}$ are the *hopping amplitudes*, $J_i \in \mathbb{R}^+$ referring to the link between sites i and $i+1$. The eigenstates of (1) can be obtained easily diagonalizing the hopping matrix J , $J_{ij} \equiv J_i \delta_{i,j+1}$. So we can write $J = U \varepsilon U^\dagger$, where ε is a diagonal matrix whose i -th entry is ε_i , the single-body energy associated to the orbital given by the i -th column of matrix U . We perform a canonical transformation, $b_k^\dagger = \sum_i U_{ki} c_i^\dagger$, such that

$$H(\mathbf{J}) = \sum_{k=1}^N \varepsilon_k b_k^\dagger b_k, \quad (2)$$

and we can write a basis of eigenstates of $H(\mathbf{J})$ by fixing the occupation numbers of the b_k^\dagger modes. Let us consider the minimum energy eigenstate with a fixed number of particles m , which is obtained by filling up the lowest m single-particle modes,

$$|\psi_m\rangle = \prod_{k=1}^m b_k^\dagger |0\rangle, \quad (3)$$

where $|0\rangle$ is the Fock vacuum. The filling fraction is defined as $\nu \equiv m/N$.

In all cases, we will assume that the sequence of hopping amplitudes presents a proper thermodynamic limit. Let $\mathbf{J}_N = \{J_{i,N}\}_{i=1}^{N-1}$ be a family of hopping amplitudes for all possible chain lengths N . Then, we assume that there exists a continuous function $J : [0,1] \mapsto \mathbb{R}^+$ such that $J_{i,N} = J(i/N)$. For concreteness, let us consider three different examples. The *Rindler metric* is the spacetime structure perceived by an observer moving with constant acceleration in a Minkowski metric, described by

$$J(x) = J_0 x. \quad (4)$$

Another natural choice is the *sine metric*,

$$J(x) = J_0 + J_1 \cos(2\pi x), \quad (5)$$

or the *rainbow metric* [9–11, 16–22], given by

$$J(x) = J_0 \exp\left(-h \left|x - \frac{1}{2}\right|\right), \quad (6)$$

for $h \geq 0$, with $h = 0$ corresponding to the Minkowski case. This metric presents a constant negative curvature except at the center [9, 18], $x = 1/2$, thus resembling an anti-de Sitter (adS) space [11], and has been extensively discussed because it presents a maximal apparent violation of the area law of the entanglement entropy. Notice that the J_0 parameter is irrelevant in all cases, since it just fixes the global energy scale, and we will take it as one.

A. Density and particle-hole symmetry

The correlation matrix can be easily computed for the GS of Hamiltonian (1),

$$C_{ij} \equiv \langle \psi_m | c_i^\dagger c_j | \psi_m \rangle = \sum_{k=1}^m \bar{U}_{ki} U_{kj}, \quad (7)$$

and, concretely, the local occupation or density is found as $\langle n_i \rangle = C_{ii}$. Since our system is bipartite, let us define an operator P acting on the single-particle wavefunctions that flips the sign of all components within one of the sublattices. It is easy to prove that $JP = -PJ$. In other terms, if U_k is an eigenstate of J with energy ε_k , then PU_k will be another eigenstate of J with energy $-\varepsilon_k$. Every negative energy orbital has a positive energy partner related through a P operation, thus proving the particle-hole symmetry of the spectrum. Since U is a unitary matrix, $\sum_{k=1}^N |U_{ki}|^2 = 1$, for all i . We may decompose the sum into two,

$$1 = \sum_{k=1}^{N/2} |U_{ki}|^2 + \sum_{k=N/2+1}^N |U_{ki}|^2, \quad (8)$$

but the second sum must be exactly the same as the first, because $|U_{k,i}|^2 = |U_{N+1-k,i}|^2$. Therefore, each sum must add up to $1/2$, thus proving that the eigenstate $|\psi_{N/2}\rangle$ at half-filling must have homogeneous occupation, $n_i = 1/2$ for all sites.

III. DEPLETION AT STRONG INHOMOGENEITY

Let us consider the strong inhomogeneity regime, in which the values of the hopping amplitudes differ largely between different links. In this situation, the strong-disorder renormalization group (SDRG) approach developed by Dasgupta and Ma describes the low-energy states very effectively [12, 23–26]. Indeed, the SDRG algorithm instructs us to select the most energetic link, J_i , and to establish a bonding or anti-bonding orbital over the corresponding couple of sites, depending on the hopping sign, which are afterwards removed from the system. Let us stress that the particle occupying such a bond has the same probability of being found on each site. The neighboring sites to this new bond are then linked among themselves by an effective hopping amplitude, which is obtained via second-order perturbation theory,

$$\tilde{J}_i = -\frac{J_L J_R}{J_i}, \quad (9)$$

where J_L and J_R are the left and right neighboring hopping amplitudes, and the minus sign is due to the

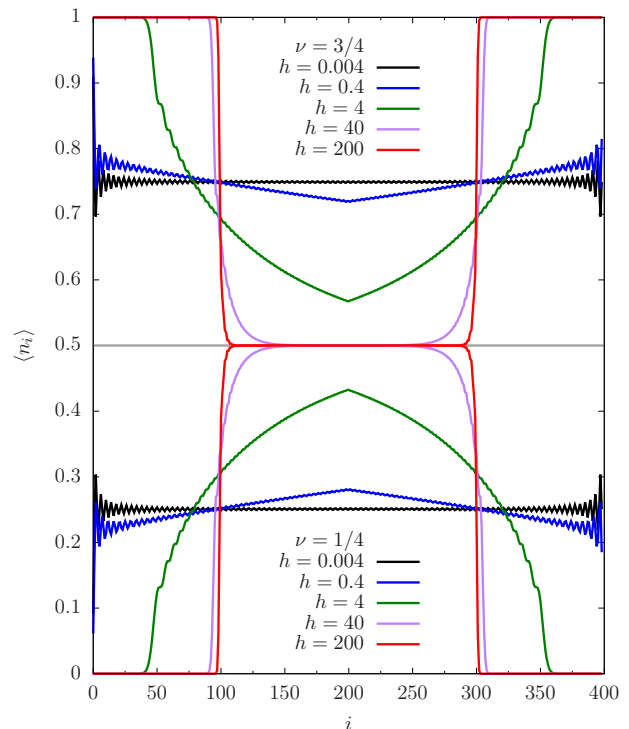


FIG. 2. Density profiles for the rainbow chain with $N = 400$ sites and two filling fractions, $\nu = 1/4$ and $\nu = 3/4$, for different values of the inhomogeneity parameter h . Notice that for low inhomogeneities we always have a nearly flat profile, which gets more modulated as the inhomogeneity increases, converging towards the SDRG prediction as the inhomogeneity becomes large. As predicted by particle-hole symmetry, the $\nu = 1/4$ and $\nu = 3/4$ cases present mirror symmetry for all the values of the inhomogeneity.

fermionic nature of the particles. Notice that this new effective link can be selected in the next iteration, if it happens to be the strongest one, thus yielding a long-distance bond. Some interesting synthetic states, such as the rainbow state, are built in such a way that all bonds (except the first one) are long-distance [16, 17].

When the SDRG algorithm is performed at half-filling we fill up $m = N/2$ bonds, each of which delocalizes a particle between a different pair of (perhaps not neighboring) sites. Thus, each site has an occupation probability of $1/2$, in accordance with the theorem of Sec. II A. Yet, if we place $m < N/2$ particles, they will always occupy the region with highest hopping amplitudes, even if the renormalization procedure yields long-distance bonds. Fig. 2 shows indeed that, in the strong inhomogeneity regime, we can observe two different density regions for $m < N/2$: half-occupied and empty. For $m > N/2$, due to particle-hole symmetry, we occupy the same bonds but in reversed order. Each site within a doubly occupied bond gets maximal occupation, $\langle n_i \rangle = 1$. Therefore, as we increase the filling fraction above $\nu = 1/2$ we fill up completely the regions with the lowest hopping amplitudes, mirroring the previous pro-

cess.

This filling sequence is illustrated in Fig. 1 (a) for a rainbow chain and (b) a dimerized chain for filling fractions $\nu = 1/2$, $\nu < 1/2$ and $\nu > 1/2$ with a small size. In Fig. 2, on the other hand, we can see the actual densities numerically obtained for a larger chain, with $N = 400$, using $\nu = 1/4$ and $\nu = 3/4$, as a function of the parameter h which controls the level of inhomogeneity. As h grows, we move from a nearly uniform density profile towards the square profile of the SDRG prediction, which differs in the cases of $\nu = 1/4$ and $\nu = 3/4$. Indeed, in both cases we have $\langle n_i \rangle = 1/2$ at the central half of the chain, while the lateral regions are depleted for $\nu = 1/4$ or full for $\nu = 3/4$.

IV. DEPLETION AT WEAK INHOMOGENEITY

In this section we establish a continuum approximation to Hamiltonian (1) for all possible filling fractions obtained through a gradient expansion. At half-filling our model is known to map into the Dirac Hamiltonian in the continuum limit,

$$i\mathcal{D}_x\psi(x) = 0, \quad (10)$$

where D_x is the covariant derivative on a given space-time metric given by the hopping function $J(x)$ [9, 18]. In this work we will consider the situation away from half-filling, showing that the gradient expansion should be taken to second order in the derivatives of the field, giving rise to a continuum approximation based on the Schrödinger equation on a curved background metric,

$$-\nabla_x^2\psi(x) + V(x)\psi(x) = E\psi(x), \quad (11)$$

where ∇_x^2 stands for the *Laplace-Beltrami* operator on a different manifold [27], whose metric is also given by the hopping function $J(x)$.

A. Dirac Hamiltonian

Let us assume that the local creation and annihilation operators can be approximated in terms of two slowly varying fermionic fields, $\psi_L(x)$ and $\psi_R(x)$, which makes reference to the right and left parts of the wavefunction,

$$\begin{aligned} c_m &= \sqrt{a} \left(e^{ik_F x} \psi_L(x) + e^{-ik_F x} \psi_R(x) \right), \\ c_m^\dagger &= \sqrt{a} \left(e^{-ik_F x} \psi_L^\dagger(x) + e^{ik_F x} \psi_R^\dagger(x) \right), \end{aligned} \quad (12)$$

where a is the lattice spacing and k_F the Fermi momentum, giving rise to the Hamiltonian

$$\begin{aligned} H(x) = - \int_0^{\mathcal{N}} dx J(x) & \left[e^{-ik_F a} \psi_L^\dagger(x+a) \psi_L(x) + e^{ik_F a} \psi_R^\dagger(x+a) \psi_R(x) \right. \\ & \left. - e^{-ik_F a} e^{-2ik_F x} \psi_L^\dagger(x+a) \psi_R(x) + e^{ik_F a} e^{2ik_F x} \psi_R^\dagger(x+a) \psi_L(x) \right], \end{aligned} \quad (13)$$

with $\mathcal{N} = Na$.

We should remark that the crossed terms, such as $\psi_L^\dagger(x+a) \psi_R(x)$, have strongly oscillating prefactors $e^{-2ik_F x}$, and thus their integral becomes negligible. As an initial approach, we may expand the fields to first order in a , $\psi(x+a) \approx \psi(x) + a\partial_x\psi(x)$, thus yielding the effective Hamiltonian

$$\begin{aligned} H(x) = - \int_0^{\mathcal{N}} dx J(x) & \left[\left(2 \cos(k_F a) - a e^{-ik_F a} \frac{J'(x)}{J(x)} \right) \psi_L^\dagger(x) \psi_L(x) \right. \\ & + \left(2 \cos(k_F a) - a e^{ik_F a} \frac{J'(x)}{J(x)} \right) \psi_R^\dagger(x) \psi_R(x) \\ & \left. + 2ai \sin(k_F a) \left(\psi_L^\dagger(x) \partial_x \psi_L(x) - \psi_R^\dagger(x) \partial_x \psi_R(x) \right) \right]. \end{aligned} \quad (14)$$

Let us perform a generic coordinate transformation, $x \rightarrow \tilde{x}$, such that

$$\frac{d\tilde{x}}{dx} = \tilde{G}(\tilde{x}), \quad (15)$$

so that $\partial_x = \tilde{G}(\tilde{x})\partial_{\tilde{x}}$, $\partial_x^2 = \tilde{G}(\tilde{x})\tilde{G}'(\tilde{x})\partial_{\tilde{x}} + \tilde{G}^2(\tilde{x})\partial_{\tilde{x}}^2$ and $\psi(x) = \tilde{\psi}(\tilde{x})\tilde{G}^{1/2}(\tilde{x})$. We will choose $\tilde{G}(\tilde{x})$ so as to make the coefficient of the first derivative homogeneous. Therefore, $\tilde{G}(\tilde{x}) = \tilde{J}(\tilde{x})$ and Eq. 14 can be written as

$$\begin{aligned}
H(\tilde{x}) = & - \int_0^{\mathcal{N}} d\tilde{x} \left[2ai \sin(k_F a) \left(\tilde{\psi}_L^\dagger \partial_{\tilde{x}} \tilde{\psi}_L(\tilde{x}) - \tilde{\psi}_R^\dagger(\tilde{x}) \partial_{\tilde{x}} \tilde{\psi}_R(\tilde{x}) \right) \right. \\
& \left. + \cos(k_F a) \left(2\tilde{J}(\tilde{x}) - a \frac{\tilde{J}'(\tilde{x})}{\tilde{J}(\tilde{x})} \right) \left(\tilde{\psi}_L^\dagger(\tilde{x}) \tilde{\psi}_L(\tilde{x}) + \tilde{\psi}_R^\dagger(\tilde{x}) \tilde{\psi}_R(\tilde{x}) \right) \right], \tag{16}
\end{aligned}$$

which in the case of half-filling, i.e. $k_F a \rightarrow \pi/2$, reduces to

$$H_D(\tilde{x}) = - \int_0^{\mathcal{N}} d\tilde{x} \, 2ai \sin(k_F a) \left(\tilde{\psi}_L^\dagger(\tilde{x}) \partial_{\tilde{x}} \tilde{\psi}_L(\tilde{x}) - \tilde{\psi}_R^\dagger(\tilde{x}) \partial_{\tilde{x}} \tilde{\psi}_R(\tilde{x}) \right). \tag{17}$$

Yet, we observe that for $k_F a < \pi/2$ the Dirac equation acquires a potential term, which may seem at first sight to be responsible for the depletion effect, but is not. Indeed, the eigenstates of (16) can be obtained in a closed form (equivalently for $\tilde{\psi}_R$),

$$\tilde{\psi}_L(\tilde{x}) = \exp \left[\frac{-i}{2a \sin(k_F a)} \left(\omega \tilde{x} - \int \cos(k_F a) \left(2\tilde{J}(\tilde{x}) - a \frac{\tilde{J}'(\tilde{x})}{\tilde{J}(\tilde{x})} \right) d\tilde{x} \right) \right], \tag{18}$$

where ω is an integration constant. In other words, the wavefunctions are modulated planes wave in \tilde{x} and they will not decay exponentially.

B. Second order approximation

In order to reproduce the observed depletion effects we should expand the fields to second order in the lattice parameter a ,

$$\psi(x+a) \approx \psi(x) + a \partial_x \psi(x) + \frac{a^2}{2} \partial_x^2 \psi(x), \tag{19}$$

thus yielding a Hamiltonian of the form

$$\begin{aligned}
H(x) = & - \int_0^{\mathcal{N}} dx J(x) \left[\left(2 \cos(k_F a) - a e^{-ik_F x} \frac{J'(x)}{J(x)} + \frac{a^2}{2} e^{-ik_F x} \frac{J''(x)}{J(x)} \right) \psi_L^\dagger(x) \psi_L(x) \right. \\
& + \left(2 \cos(k_F a) - a e^{ik_F x} \frac{J'(x)}{J(x)} + \frac{a^2}{2} e^{ik_F x} \frac{J''(x)}{J(x)} \right) \psi_R^\dagger(x) \psi_R(x) \\
& + 2ai \sin(k_F a) \left(\psi_L^\dagger(x) \partial_x \psi_L(x) - \psi_R^\dagger(x) \partial_x \psi_R(x) \right) \\
& + a^2 e^{ik_F x} \frac{J'(x)}{J(x)} \psi_R^\dagger(x) \partial_x \psi_R(x) + a^2 e^{-ik_F x} \frac{J'(x)}{J(x)} \psi_L^\dagger(x) \partial_x \psi_L(x) \\
& \left. + a^2 \cos(k_F a) \left(\psi_L^\dagger(x) \partial_x^2 \psi_L(x) + \psi_R^\dagger(x) \partial_x^2 \psi_R(x) \right) \right], \tag{20}
\end{aligned}$$

which gives rise to the following equations of motion,

$$\begin{aligned}
E\psi(x)_{R/L} = & -J(x) \left[\left(2 \cos(k_F a) - a e^{\pm ik_F a} \frac{J'(x)}{J(x)} + \frac{a^2}{2} e^{\pm ik_F a} \frac{J''(x)}{J(x)} \right) \psi(x)_{R/L} \right. \\
& \mp 2ai \sin(k_F a) \partial_x \psi(x)_{R/L} + a^2 e^{\pm ik_F a} \frac{J'(x)}{J(x)} \partial_x \psi(x)_{R/L} \\
& \left. + a^2 \cos(k_F a) \partial_x^2 \psi(x)_{R/L} \right], \tag{21}
\end{aligned}$$

where the R/L notation makes reference to the right and left parts of the wavefunction, and the corresponding sign should be chosen in each case. We would like to notice that a second-order discrete version of Eq. (21) with lattice spacing a yields our original single-body Hamiltonian (1), thus proving the direct equivalence between both systems.

In the rest of the section we will transform this equation into a Schrödinger equation, making use of two transformations: (a) a coordinate transformation following Eq. 15, which is equivalent to embedding our system in a non-trivial space-time metric, and (b) a gauge transformation in order to get rid of the first derivative term.

Our next purpose is then to make the coefficient of the second derivative homogeneous through a suitable change of variable \tilde{x} . Making a slight abuse of notation, we let $\tilde{J}(\tilde{x})\tilde{G}^2(\tilde{x}) = 1 \rightarrow \tilde{G}(\tilde{x}) = \tilde{J}^{-1/2}(\tilde{x})$. Notice the difference with Eq. 14, in which we had $\tilde{G}(\tilde{x}) = \tilde{J}(\tilde{x})$ once the appropriate transformation of coordinates was performed in order to obtain a homogeneous first-derivative term. The equation of motion in these new transformed coordinates reads

$$\begin{aligned} E\tilde{\psi}(\tilde{x})_{R/L} = & -a^2 \cos(k_F a) \partial_{\tilde{x}}^2 \tilde{\psi}(\tilde{x})_{R/L} \pm 2i \sin(k_F a) \left(a\tilde{J}^{1/2}(\tilde{x}) - \frac{a^2}{2} \frac{\tilde{J}'(\tilde{x})}{\tilde{J}(\tilde{x})} \right) \partial_{\tilde{x}} \tilde{\psi}(\tilde{x})_{R/L} \\ & - 2 \cos(k_F a) \left(\tilde{J}(\tilde{x}) - \frac{a}{4} \frac{\tilde{J}'(\tilde{x})}{\tilde{J}^{1/2}(\tilde{x})} + \frac{7a^2}{32} \frac{\tilde{J}^2(\tilde{x})}{\tilde{J}^2(\tilde{x})} - \frac{a^2}{8} \frac{\tilde{J}''(\tilde{x})}{\tilde{J}(\tilde{x})} \right) \tilde{\psi}(\tilde{x})_{R/L} \\ & - \frac{e^{\pm i k_F a}}{2} \left(-a \frac{\tilde{J}'(\tilde{x})}{\tilde{J}^{1/2}(\tilde{x})} - a^2 \frac{\tilde{J}'^2(\tilde{x})}{\tilde{J}^2(\tilde{x})} + a^2 \frac{\tilde{J}''(\tilde{x})}{\tilde{J}(\tilde{x})} \right) \tilde{\psi}(\tilde{x})_{R/L}. \end{aligned} \quad (22)$$

This equation can be rewritten so as to make the single-body operator manifestly hermitean,

$$\begin{aligned} E\tilde{\psi}(\tilde{x})_{R/L} = & -a^2 \cos(k_F a) \partial_{\tilde{x}}^2 \tilde{\psi}(\tilde{x})_{R/L} \\ & \pm 2i \sin(k_F a) \left(a\tilde{J}^{1/4}(\tilde{x}) \partial_{\tilde{x}} \left(\tilde{J}^{1/4}(\tilde{x}) \tilde{\psi}(\tilde{x})_{R/L} \right) - \frac{a^2}{2} \left(\frac{\tilde{J}'(\tilde{x})}{\tilde{J}(\tilde{x})} \right)^{1/2} \partial_{\tilde{x}} \left(\frac{\tilde{J}'(\tilde{x})}{\tilde{J}(\tilde{x})} \right)^{1/2} \tilde{\psi}(\tilde{x})_{R/L} \right) \\ & - 2 \cos(k_F a) \left(\tilde{J}(\tilde{x}) - \frac{a}{2} \frac{\tilde{J}'(\tilde{x})}{\tilde{J}^{1/2}(\tilde{x})} - \frac{a^2}{32} \frac{\tilde{J}'^2(\tilde{x})}{\tilde{J}^2(\tilde{x})} + \frac{a^2}{8} \frac{\tilde{J}''(\tilde{x})}{\tilde{J}(\tilde{x})} \right) \tilde{\psi}(\tilde{x})_{R/L}. \end{aligned} \quad (23)$$

In order to transform our equation of motion into a Schrödinger equation, our next task is to get rid of the first derivative term using a gauge transformation,

$$\tilde{\psi}(\tilde{x})_{R/L} = e^{i\beta_{R/L}(\tilde{x})} \tilde{\Psi}(\tilde{x})_{R/L}, \quad (24)$$

which implies that

$$\begin{aligned} \partial_{\tilde{x}} \tilde{\psi}(\tilde{x})_{R/L} &= i\beta'_{R/L}(\tilde{x}) e^{i\beta_{R/L}(\tilde{x})} \tilde{\Psi}(\tilde{x})_{R/L} + e^{i\beta_{R/L}(\tilde{x})} \partial_{\tilde{x}} \tilde{\Psi}(\tilde{x})_{R/L}, \\ \partial_{\tilde{x}}^2 \tilde{\psi}(\tilde{x})_{R/L} &= i\beta''_{R/L}(\tilde{x}) e^{i\beta_{R/L}(\tilde{x})} \tilde{\Psi}(\tilde{x})_{R/L} - \beta'^2_{R/L}(\tilde{x}) e^{i\beta_{R/L}(\tilde{x})} \tilde{\Psi}(\tilde{x})_{R/L} + 2i\beta'_{R/L}(\tilde{x}) e^{i\beta_{R/L}(\tilde{x})} \partial_{\tilde{x}} \tilde{\Psi}(\tilde{x})_{R/L} \\ &\quad + e^{i\beta_{R/L}(\tilde{x})} \partial_{\tilde{x}}^2 \tilde{\Psi}(\tilde{x})_{R/L}. \end{aligned} \quad (25)$$

The condition that we have to impose so that the first-derivative terms cancel out is

$$\beta'_{R/L}(\tilde{x}) = \mp \tan(k_F a) \left(\frac{1}{2} \frac{\tilde{J}'(\tilde{x})}{\tilde{J}(\tilde{x})} - \frac{1}{a} \tilde{J}^{1/2}(\tilde{x}) \right). \quad (26)$$

Applying this transformation we obtain

$$\begin{aligned} E\tilde{\Psi}(\tilde{x})_{R/L} = & -\frac{1 + \cos^2(k_F a)}{\cos(k_F a)} \tilde{J}(\tilde{x}) \tilde{\Psi}(\tilde{x})_{R/L} \\ & + a \frac{1}{\cos(k_F a)} \frac{\tilde{J}'(\tilde{x})}{\tilde{J}^{1/2}(\tilde{x})} \tilde{\Psi}(\tilde{x})_{R/L} \\ & - \frac{a^2}{4} \left(\frac{\sin(k_F a)^2}{\cos(k_F a)} \frac{\tilde{J}'^2(\tilde{x})}{\tilde{J}^2(\tilde{x})} - \frac{\cos(k_F a)}{4} \frac{\tilde{J}'^2(\tilde{x})}{\tilde{J}^2(\tilde{x})} + \cos(k_F a) \frac{\tilde{J}''(\tilde{x})}{\tilde{J}(\tilde{x})} \right) \tilde{\Psi}(\tilde{x})_{R/L} \\ & - a^2 \cos(k_F a) \partial_{\tilde{x}}^2 \tilde{\Psi}(\tilde{x})_{R/L}. \end{aligned} \quad (27)$$

Eq. (27) has the form of a Schrödinger equation in \tilde{x} with a mass $M = 2/\cos(k_F a)$ that tends to zero as

$k_F a \rightarrow \pi/2$, thus rendering the approximation invalid in that limit. The effective potential, to zero order in a , becomes

$$V(\tilde{x}) \approx -\frac{1 + \cos^2(k_F a)}{\cos(k_F a)} \tilde{J}(\tilde{x}). \quad (28)$$

Notice that, for $k_F a \ll 1$ we have to a very good approximation $V(\tilde{x}) \approx -2\tilde{J}(\tilde{x})$ or, equivalently, $V(x) = -2J(x)$, while for larger values of $k_F a$ the different modes of our system correspond to different Schrödinger equations. The reason is that the prefactors of Eq. (27) present explicit dependence on $k_F a$. The next corrections, corresponding to higher orders in a , can be shown to be small or constant for the hopping amplitudes employed in this work. We would also like to stress that our system is now embedded on a manifold with metric $ds^2 = dt^2 - d\tilde{x}^2$, and all geometrical measurements should be transformed back before further comparisons with our original discrete model.

Let us discuss the numerical validity of Eq. (27), which is familiar to us due to its Schrödinger form. For highly excited states we are allowed to perform a Wentzel-Kramers-Brillouin (WKB) approximation, which leads to a form

$$\tilde{\Psi}(\tilde{x})_{R/L} \sim \frac{1}{\sqrt{\tilde{p}(\tilde{x})}} e^{\pm i\tilde{p}(\tilde{x})\tilde{x}}, \quad (29)$$

in the new coordinate \tilde{x} , where $\tilde{p}(\tilde{x})$ is the momentum of a particle in that position according to classical mechanics, i.e. $p(x) = \pm\sqrt{2M(E - V(x))}$

$$\tilde{p}(\tilde{x}) = \sqrt{\frac{1}{\cos^2(k_F a)} \left(\frac{1 + \cos^2(k_F a)}{\cos(k_F a)} \tilde{J}(\tilde{x}) + E \right)}, \quad (30)$$

Yet, we should transform this solution back to our original coordinate system in order to check its numerical validity, making use of the change of coordinates for a probability distribution, $|\tilde{\Psi}(\tilde{x})|^2 d\tilde{x} = |\Psi(x)|^2 dx$, which leads to

$$|\Psi(x)_{R/L}| = \frac{|\tilde{\Psi}(\tilde{x})_{R/L}|}{J^{1/4}(\tilde{x})} \sim \frac{1}{\sqrt{\tilde{p}(\tilde{x})}} \frac{1}{J^{1/4}(\tilde{x})}. \quad (31)$$

We have checked the validity of Eq. (31) in Fig. 3. In panel (a) we have chosen a Rindler system with $J(x) = \frac{1}{4} + x$ with $N = 400$ and shown the modes $m = 50, 100$ and 175 . The continuous red curve in each case corresponds to the approximation (31), suitably normalized. We can see that the decay is nearly perfect. Panel (b) shows the same situation for the rainbow chain, using $h = 4$, $N = 400$, with the modes $m = 40$ and $m = 150$. We can see that the decay is nearly perfect in all the cases.

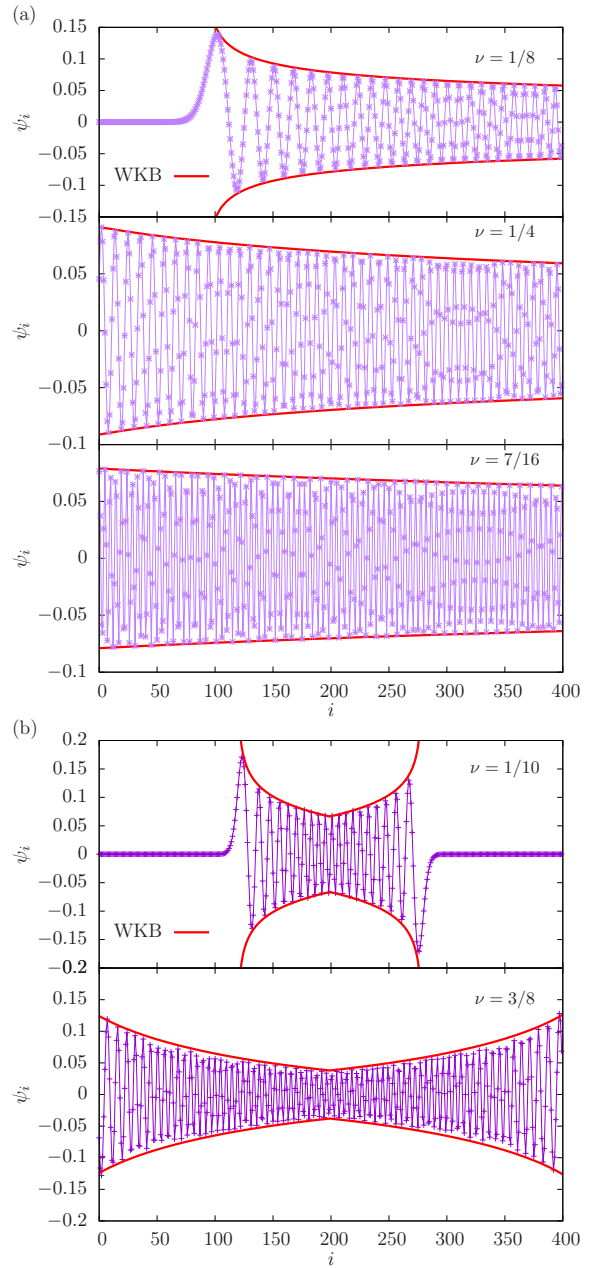


FIG. 3. Comparing the modes obtained from Hamiltonian (1) using $N = 400$ for Rindler and Rainbow chains with the WKB approximation given in Eq. (31), considering different filling fractions ν . The continuous red line represents the semiclassical approximation Eq. (31) to the continuous approximation given in Eq. (27). Panel (a): Rindler chain, from top to bottom, $m = 50, 100$ and 175 . Panel (b): rainbow chain, top to bottom $m = 40$ and $m = 150$.

We should stress that our continuum approximation, Eq. (33) can not be employed to obtain a continuum limit of our original model. Indeed, for $a \rightarrow 0$, all terms containing derivatives of the field $\psi(x)$ vanish, thus rendering the equation useless. In order to make sense of Eq. (33) we must keep a finite and this implies that we should preserve all derivatives of the gradient expan-

sion. Alternatively, we may define a new physical variable $u = x/a$, in such a way that any derivative with respect to x multiplied by a becomes a derivative with respect to u : $\partial_u = a\partial_x$.

V. DENSITY PROFILES

Our next aim will be to provide a continuum approximation to the density profiles observed for free-fermionic chains with inhomogeneous hopping amplitudes away from half-filling, based on the validity of the Schrödinger equation on a different manifold, Eq. (27), using a certain effective potential $V(x)$. If we fill all orbitals up to a certain energy E , we will observe depletion in the classically forbidden regions, defined by $V(x) > E$, and bounded by the turning points, defined by $V(x_*) = E$. To order zero in a , from (28), we may estimate these turning points as

$$E = -\frac{1 + \cos^2(k_F a)}{\cos(k_F a)} J(x_*). \quad (32)$$

This result can also be obtained in a heuristic way, starting from a simplified version of Eq. (21),

$$\begin{aligned} E\psi(x)_{R/L} &= -J(x) (2 \cos(k_F a) \psi(x)_{R/L} \\ &\quad \mp 2ai \sin(k_F a) \partial_x \psi(x)_{R/L} \\ &\quad + a^2 \cos(k_F a) \partial_x^2 \psi(x)_{R/L}). \end{aligned} \quad (33)$$

Now, we suppose that the wavefunction is locally a plane wave with a certain position dependent momentum $q(x)$, i.e. $\psi(x)_{R/L} \sim e^{\pm iq(x)x}$. Then,

$$\begin{aligned} E &= -J(x)(2 \cos(k_F a) + 2a \sin(k_F a)q(x) \\ &\quad - a^2 \cos(k_F a)q(x)^2), \end{aligned} \quad (34)$$

and we can then obtain $q(x)$ solving a quadratic equation. If $q(x)$ is not real, then x belongs to the classically forbidden region. Thus, by making the discriminant zero we reach Eq. 32.

We can obtain an approximation to the local density $\rho(x)$ of a Schrödinger equation by considering a particle with energy E traveling through a small segment of size Δx around position x , where the potential energy is $V(x)$. Its momentum will be given by

$$q(x) = \sqrt{2m(E - V(x))}. \quad (35)$$

Within a semiclassical approximation we may estimate the number of orbitals with presence on that segment assuming that the momenta are discretized as $q(x) \approx n\pi/N \approx \pi\rho(x)$. Thus, we have

$$\rho(x) \approx \frac{1}{\pi} \sqrt{2m(E - V(x))}. \quad (36)$$

In our case, for low values of $k_F a$ we also build the density by filling up the modes of a Schrödinger equation, and thus we may write

$$\tilde{\rho}(\tilde{x}) \approx \frac{1}{\pi} \sqrt{\frac{2}{a^2} (E - 2\tilde{J}(\tilde{x}))}. \quad (37)$$

Yet, this expression is designed for the transformed coordinate \tilde{x} . We should express it in our original coordinate in order to make useful predictions, using $\tilde{\rho}(\tilde{x})d\tilde{x} = \rho(x)dx$, we have $\rho(x) = \tilde{\rho}(\tilde{x})\tilde{J}^{-1/2}(\tilde{x})$, and therefore

$$\rho(x)a \approx A \sqrt{\frac{E}{J(x)} - 2}, \quad (38)$$

where A is a normalization constant. Indeed, $\rho(x)a$ can be interpreted as the local occupation, which can be directly compared to $\langle c_i^\dagger c_i \rangle$ for $i = x/a$. Interestingly, the density is directly related to the *inverse* of the hopping function $J(x)$. Notice that Eq. (38) is not necessarily valid for larger values of $k_F a$, since the modes that we are filling up do not correspond to the same Schrödinger equation.

We have computed numerically the fermionic density for different hopping functions, and observed depletion in all the considered cases, except for the Minkowski space-time, as we can see in Fig. 4. As expected, the depleted regions decrease their size as the filling fraction grows. Moreover, Eq. (38) predicts very well the density profiles for all $\nu \leq 1/4$. Surprisingly, for all values of the filling fraction the functional form

$$\rho(x)a = A \sqrt{\frac{1}{J(x)} - B}, \quad (39)$$

fits extremely well the numerical density profiles, as we can check in Fig. 4.

VI. COMPENSATING AND MIMICKING POTENTIALS

As we have discussed above, our continuum approximation led to an effective Schrödinger equation with a potential whose classically forbidden areas correspond to the depletion regions of the particle density.

Let us extend our original model, Eq. (1), introducing an inhomogeneous chemical potential $\boldsymbol{\mu} = \{\mu_i\}_{i=1}^N$,

$$H(\mathbf{J}, \boldsymbol{\mu})_N = - \sum_{i=1}^{N-1} J_i (c_i^\dagger c_{i+1} + \text{h.c.}) + \sum_{i=1}^N \mu_i c_i^\dagger c_i. \quad (40)$$

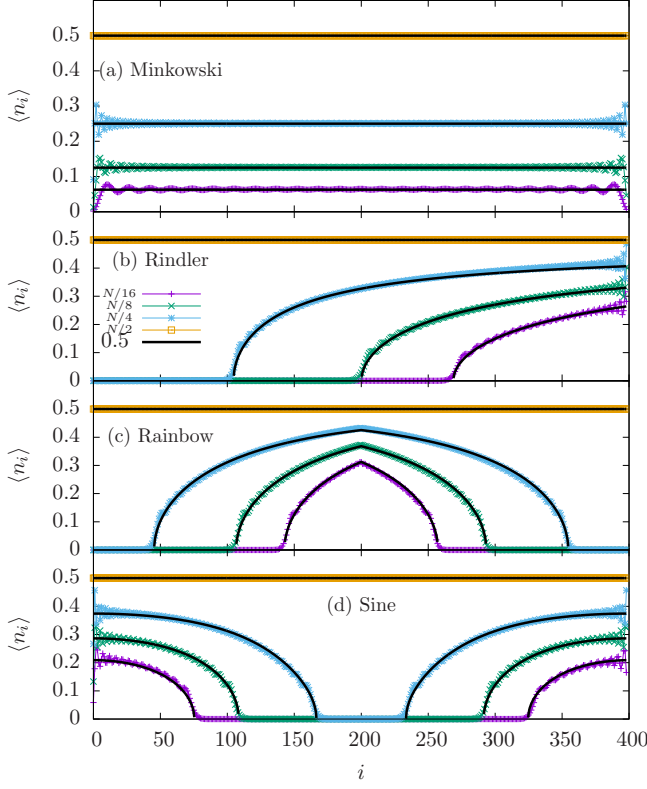


FIG. 4. Fermionic density for a chain of $N = 400$ sites with different filling fractions $1/2, 1/4, 1/8$ and $1/16$ and four different inhomogeneities: (a) Minkowski, (b) Rindler, $J(x) = x$, (c) Rainbow, $J(x) = \exp(-h|x - 1/2|)$ with $h = 0.01$ and (d) Sine, $J(x) = 1 + 0.5 \cos(2\pi x)$. The black curves correspond to the theoretical curves, given by Eq. (38).

We may introduce a *compensating potential*, defined by

$$\mu_i = \mu_0 J_i, \quad (41)$$

where we implicitly assume that the chemical potential at site i is given by the average of its two neighboring hopping constants. With such choice, the GS of Hamiltonian (40) always presents a flat density profile, for all filling fractions, whenever $\mu_0 = 2 \cos(k_F a)$, as it can be checked in Fig. 5. In mathematical terms, the reason is that the added chemical potential cancels out the potential energy term in Eq. (21). In this case the Hamiltonian does not present any terms which are independent of the lattice spacing, a , and thus we are allowed to renormalize the hopping function, $J(x) \rightarrow \infty$, $a \rightarrow 0$, while $J(x)a \rightarrow \hat{J}(x)$, thus yielding a proper continuum limit.

The physical meaning of this compensating effect is also interesting. Let us start out with the GS of Hamiltonian (40) using $J_i = 1$ and $\mu_i = 0$, filled up with νN fermions. We notice that the energy cost of introducing a new particle does not decay to zero as the system size increases, and instead is bounded by $-2 \cos(k_F a)$, with

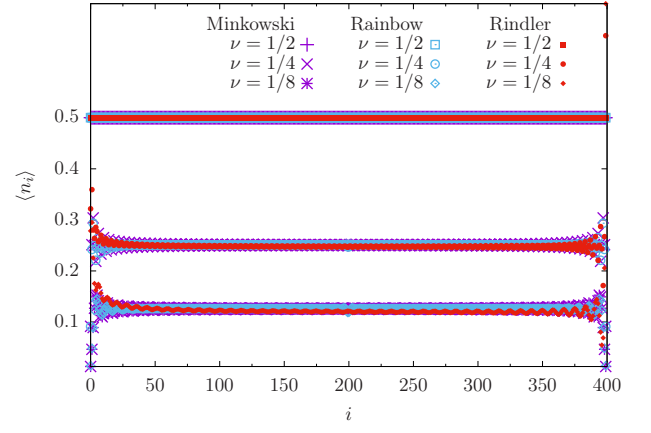


FIG. 5. Density profile for the GS of Hamiltonian (40) with a compensating potential, using three types of hopping functions: Minkowski, Rindler and rainbow, and different filling fractions, $\nu = 1/2, 1/4$ and $1/8$.

$k_F a = \pi \nu$. Thus, the system can not be conformally invariant. We can change that by introducing a chemical potential, $\mu_i = 2 \cos(k_F a)$. In that case, the energy cost of introducing extra particles becomes zero. This new system can be set in any different static 1+1D metric by introducing an appropriate Weyl factor, thus yielding the compensating potential system [9, 22].

Now we may ask a complementary question. Let us keep a flat hopping function, $J(x) = 1$, i.e. $J_i = 1$. Can we find a chemical potential $\{\mu_i\}$ which *mimics* the density profiles obtained from the inhomogeneous hopping function without chemical potential, for the same filling fraction? Interestingly, the answer is yes.

Let us consider the bulk equations to obtain the eigenstates of the original hopping matrix. Let $(\psi_1 \cdots \psi_N)^T$ be the eigenvector of the hopping matrix with eigenvalue E . Then,

$$J_{n-1} \psi_{n-1} + J_n \psi_{n+1} = E \psi_n, \quad (42)$$

which can be rewritten for very smooth \mathbf{J} as

$$J_n (\psi_{n-1} + \psi_{n+1}) \approx E \psi_n. \quad (43)$$

Now we can take the hopping amplitude to the RHS, assuming that it is non-zero,

$$\psi_{n-1} + \psi_{n+1} - \left(\frac{E}{J_n} - E \right) \psi_n \approx E \psi_n, \quad (44)$$

which can be read as a homogeneous hopping Hamiltonian with a chemical potential μ_n of the form

$$\mu_n = E \left(\frac{1}{J_n} - 1 \right), \quad (45)$$

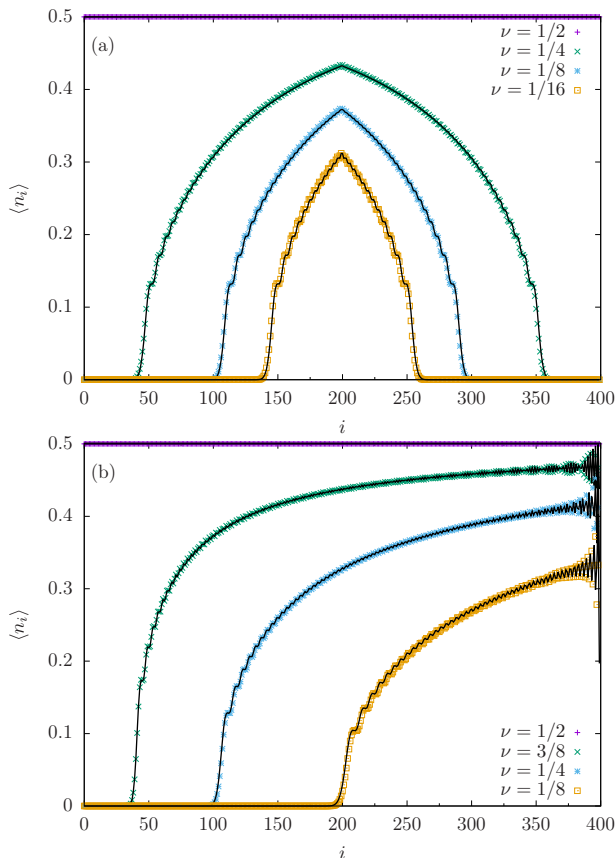


FIG. 6. Density profiles of the GS of Hamiltonian (40) using homogeneous hoppings, $J_i = 1$, and the corresponding mimicking potential, Eq. (46), for (a) a rainbow chain with $N = 400$ and $h = 4$ and (b) a Rindler system with $J(x) = x$, using the filling fractions shown in the key, along with the original density profiles using inhomogeneous hoppings and without chemical potential.

i.e. the chemical potential depends on the energy itself, and thus the secular equation becomes non-linear. This reasoning motivates the following *mimicking* chemical potential

$$\mu_i = \frac{\mu_0}{J_i} \quad (46)$$

In Fig. 6 we plot the density profiles associated to the ground states of Eq. (40) with the above chemical potential Eq. (46), along with the original density profiles obtained for inhomogeneous hoppings and without chemical potential. The coincidence between them both is extremely remarkable, given that Eq. (46) only ensures the similarity between the highest energy filled mode in both cases.

Thus, we are led to ask whether the two GS are the same or not. Fig. 7 provides a negative answer to that question. In it we have shown the entanglement entropies (EE) of blocks $A = [1, \dots, \ell]$ as a function of ℓ for both states in the rainbow case, defined as

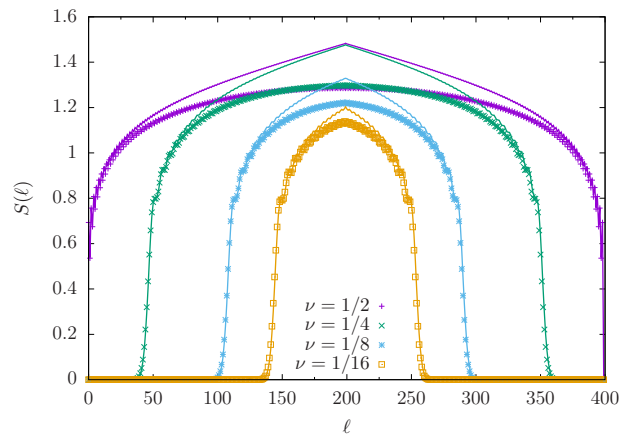


FIG. 7. Entanglement entropy $S(\ell)$ of blocks of the form $[1, \dots, \ell]$ of the mimicking GS (points) and the original GS (lines), with the same filling fractions for rainbow chains with $h = 4$ and $N = 400$.

$S(\ell) = -\text{Tr}_A(\rho_A \log \rho_A)$ with $\rho_A = \text{Tr}_{\bar{A}} |\Psi\rangle \langle \Psi|$. As it was shown in [13], the EE of our states is approximately equal to the EE of blocks of a shorter system bounded by the turning points at half-filling [9, 22]. Yet, the EE of the GS of the mimicking system are different, presenting strong similarities to the EE of homogeneous chains [28].

VII. CONCLUSIONS AND FURTHER WORK

A free-fermionic chain without chemical potential and with inhomogeneous hoppings at half-filling will present an exactly homogeneous density profile. In the continuum limit, this system represents a Dirac fermion on a static curved background, with the lapse function of the metric given by the hopping amplitudes. Yet, if we move away from half-filling we will notice that the particles concentrate at the regions with higher hopping amplitudes, and leave the regions with lower hopping amplitudes empty, a phenomenon that we have called *depletion*.

In the strong inhomogeneity regime, the Dasgupta-Ma renormalization scheme allows to prove that this should be the case, since the particles will establish bonds on top of the larger hoppings, either original or renormalized. Thus, the depletion is exact.

In the weak inhomogeneity regime, we have shown that the associated single-particle problem is equivalent to a Schrödinger equation on a different static curved manifold, with the lapse function given by the *square root* of the hopping amplitudes, and a potential determined by the hopping amplitudes and the filling fraction. Notice that this shows that the effective system does not show conformal invariance. Naturally, the laplacian operator must be substituted with the Laplace-Beltrami operator corresponding to the associated metric, and the depleted regions correspond to the classically forbidden areas of this Schrödinger equation. The wavefunctions and the

density profiles can be accurately obtained using a semi-classical approximation.

It is interesting to ask how this model breaks the conformal symmetry which is known to hold at half-filling. Indeed, a second order expansion of the fields is required to find a continuum approximation to our lattice model, instead of the first-order expansion at half-filling. The second-order derivative term, which maps into a laplacian, breaks explicitly the conformal invariance introducing a length scale, which is inversely proportional to the effective mass.

We may introduce a *compensating potential* in our system, through a chemical potential proportional to the hopping amplitudes, which exactly cancels the depletion effect and provides exactly homogeneous density profiles. In this case, the continuous approximation allows us to conjecture that the system recovers its full conformal invariance.

We have also introduced a *mimicking potential*, which provides exactly the same density profiles away from half filling on a fermionic chain with homogeneous hoppings. Interestingly, this mimicking potential is inversely proportional to the hopping amplitudes. Yet, the associated ground state is not the same as in the original case, as we have been able to show checking the entanglement

entropies of lateral blocks. The ground states of the compensating and mimicking systems present interesting challenges which should be considered in further work.

ACKNOWLEDGMENTS

We would like to acknowledge very useful discussions with E. Tonni, A. González-López, F. Finkel and J.E. Alvarellos. This work was funded by the Spanish government through grants PGC2018-095862-B-C21, PGC2018-094763-B-I00, PID2019-105182GB-I00, QUITEMAD+ S2013/ICE-2801, SEV-2016-0597 of the “Centro de Excelencia Severo Ochoa” Programme and the CSIC Research Platform on Quantum Technologies PTI-001, and by Comunidad de Madrid (Spain) under the Multiannual Agreement with UC3M in the line of Excellence of University Professors (EPUC3M14 and EPUC3M23), in the context of the V Plan Regional de Investigación Científica e Innovación Tecnológica (PRICIT). B.M. acknowledges financial support through contract No. 2022/167 under the EPUC3M23 line. N.S. acknowledges the financial support from QTP2021-03-009 QTEP from the Recovery, Transformation and Resilience Plan (RTRP) national program.

-
- [1] F. Schäfer, T. Fukuhara, S. Sugawa, Y. Takasu, Y. Takahashi, *Tools for quantum simulation with ultracold atoms in optical lattices*, Nature Rev. Phys. **2**, 411 (2020).
 - [2] C. Gross, I. Bloch, *Quantum simulations with ultracold atoms in optical lattices*, Science **357**, 995 (2017).
 - [3] O. Boada, A. Celi, J.I. Latorre, M. Lewenstein, *Dirac equation for cold atoms in artificial curved spacetimes*, New J. Phys. **13**, 035002 (2011).
 - [4] J. Rodríguez-Laguna, L. Tarruell, M. Lewenstein, A. Celi, *Synthetic Unruh effect in cold atoms*, Phys. Rev. A **95**, 013627 (2017).
 - [5] B. Mula, S.N. Santalla, J. Rodríguez-Laguna, *Casimir forces on deformed fermionic chains*, Phys. Rev. Res. **3**, 013062(9) (2021).
 - [6] M. Lewenstein, A. Sanpera, V. Ahufinger, *Ultracold atoms in optical lattices*, Oxford University Press (2012).
 - [7] P. di Francesco, P. Matthieu, D. Sénéchal, *Conformal Field Theory*, Springer (1997).
 - [8] G. Mussardo, *Statistical Field Theory*, Oxford Graduate Texts (2010).
 - [9] J. Rodríguez-Laguna, J. Dubaïl, G. Ramírez, P. Calabrese, G. Sierra, *More on the rainbow chain: entanglement, space-time geometry and thermal states*, J. Phys. A **50**, 164001 (2017).
 - [10] E. Tonni, J. Rodríguez-Laguna, G. Sierra, *Entanglement hamiltonian and entanglement contour in inhomogeneous 1D critical systems*, J. Stat. Mech. 043105 (2018).
 - [11] I. MacCormack, A.L. Liu, M. Nozaki, S. Ryu, *Holographic Duals of Inhomogeneous Systems: The Rainbow Chain and the Sine-Square Deformation Model*, J. Phys. A: Math. and Theor. **52**, 505401 (2019).
 - [12] C. Dasgupta, S.-K. Ma, *Low-temperature properties of the random Heisenberg antiferromagnetic chain*, Phys. Rev. B **22**, 1305 (1980).
 - [13] F. Finkel, A. González-López, *Entanglement entropy of inhomogeneous XX spin chains with algebraic interactions*, J. High Energy Phys. 184(35) (2021).
 - [14] L. Dagure, R. Medina, M. Solís, G. Torroba, *Aspects of quantum information in finite density field theory*, JHEP 079 (2021).
 - [15] M. Mintchev, D. Pontello, A. Sartori, E. Tonni, *Entanglement entropies of an interval in the free Schrödinger field theory at finite density*, JHEP 120 (2022).
 - [16] G. Vitagliano, A. Riera, J.I. Latorre, *Volume-law scaling for the entanglement entropy in spin-1/2 chains*, New J. of Phys. **12**, 113049 (2010).
 - [17] G. Ramirez, J. Rodriguez-Laguna, G. Sierra, *From conformal to volume-law for the entanglement entropy in exponentially deformed critical spin 1/2 chains*, J. Stat. Mech. P10004 (2014).
 - [18] G. Ramirez, J. Rodriguez-Laguna, G. Sierra, *Entanglement over the rainbow*, J. Stat. Mech. P06002 (2015).
 - [19] J. Rodríguez-Laguna, S.N. Santalla, G. Ramirez, G. Sierra, *Entanglement in correlated random spin chains, RNA folding and kinetic roughening*, New J. Phys. **18**, 073025 (2016).
 - [20] N. Samos Sáenz de Buruaga, S.N. Santalla, J. Rodríguez-Laguna, G. Sierra, *Symmetry protected phases in inhomogeneous spin chains*, J. Stat. Mech. 093102 (2019).
 - [21] N. Samos Sáenz de Buruaga, S.N. Santalla, J. Rodríguez-Laguna, G. Sierra, *Piercing the rainbow: entanglement on an inhomogeneous spin chain with a defect*, Phys. Rev. B **101**, 205121 (2020).
 - [22] N. Samos Sáenz de Buruaga, S.N. Santalla, J. Rodríguez-

- Laguna, G. Sierra, *Entanglement in non-critical inhomogeneous quantum chains*, Phys. Rev. B **104**, 195147 (2021).
- [23] G. Refael, J.E. Moore, *Entanglement entropy of random quantum critical points in one dimension*, Phys. Rev. Lett. **93**, 260602 (2004).
- [24] N. Laflorencie, *Scaling of entanglement entropy in the random singlet phase*, Phys. Rev. B **72**, 140408(R) (2005).
- [25] A. Hoyos, A.P. Vieira, N. Laflorencie, E. Miranda, *Correlation amplitude and entanglement entropy in random spin chains*, Phys. Rev. B **76**, 174425 (2007).
- [26] G. Ramírez, J. Rodríguez-Laguna, G. Sierra, *Entanglement in low-energy states of the random-hopping model*, J. Stat. Mech. P07003 (2014).
- [27] S. Rosenberg, *The laplacian on a riemannian manifold*, Cambridge Univ. Press (2009).
- [28] P. Calabrese, J.L. Cardy, *Entanglement entropy and quantum field theory*, JSTAT P06002 (2004).
- [29] M. Fagotti, P. Calabrese, *Universal parity effects in the entanglement entropy of XX chains with open boundary conditions*, J. Stat. Mech. P01017 (2011)